Soliton and phonon production by an oscillating obstacle in a quasi-one-dimensional trapped repulsive Bose-Einstein condensate

Abdelaziz Radouani*
Laboratoire de Physique Statistique, Ecole Normale Supérieure, 24 rue Lhomond, 75231 Paris Cedex 05, France and Laboratoire de Biophysique, Faculté de Médecine et de Pharmacie, Rabat, Morocco
(Received 20 November 2003; published 1 July 2004)

We use the one-dimensional (1D) Gross-Pitaevskii equation to investigate the dynamical evolution of a dilute repulsive Bose-Einstein condensate (BEC) confined in an elongated static nonharmonic trap and stirred by an oscillating Gaussian obstacle moving at uniform speed in alternate direction. Direct numerical solutions of this equation show that above a critical obstacle velocity, the motion of the obstacle creates gray solitons and phonons. At first, when the velocity of the obstacle increases, the dissipation also increases. But the dissipation reaches a maximal value and then decreases dramatically and vanishes at high obstacle velocities. Our results at low obstacle velocities are similar to those previously obtained experimentally and by simulations in the case of vortice and phonon production in 3D and 2D trapped repulsive BEC's. But at high obstacle velocities, we show that the quasi-1D trapped repulsive BEC behaves as a quasisuperfluid medium with disappearance of gray soliton and phonon excitations. This extends previous results and provides the main dependence of the phenomenon on the obstacle characteristics.

DOI: 10.1103/PhysRevA.70.013602 PACS number(s): 03.75.Kk

I. INTRODUCTION

Since the discovery of superfluidity in helium II [1], intensive experimental and theoretical efforts have been devoted to the investigation of elementary excitations and superfluidity in quantum Bose gases. Remarkable developments in this field have led to new concepts such as the critical velocity first introduced by Landau [2] in his famous criterion, phonons and speed of sound predicted by Bogoliubov [3], quantized vortices proposed by Feynman [4], and others. However, strong interparticle interactions within superfluid liquid helium, plus thermal and quantum fluctuations, impede the formulation of a satisfactory microscopic theory that can be able to explain from first principles the mechanism of superfluidity and production of vortices in liquid helium.

With the successful experimental realization of Bose-Einstein condensates (BEC's) [5–7] in trapped dilute alkali vapors, remarkable experimental studies of the dynamical properties of BEC's have been performed. In particular, important features of these condensates were found in the MIT experiment on the interference of two independently prepared condensates [8]. In the JILA experiment [9] in a dilute and almost pure BEC at zero temperature ($T=0$), it was found that only binary elastic interparticle collisions are relevant and can be characterized by a single parameter: the s-wave scattering length denoted a. These latter results have constituted a direct verification of the Bogoliubov approach of weakly interacting Bose gases [3] and justified the use of the mean-field approximation to model the dynamical and quantum properties of a dilute BEC near zero temperature. A very remarkable consequence is that the time evolution of such a condensate wave function can be accurately described by the nonlinear Schrödinger equation (NLSE), also known as the Gross-Pitaevskii equation (GPE) [10]. This has allowed for direct quantitative comparisons between theory and experiment [12]. The stability of large BEC's requires repulsive interparticle interactions (positive a).

Two different directions have recently attracted particular interest. One of them is the study of BEC's in reduced dimensionality. Indeed, development of the trapping techniques has allowed for the realization of very anisotropic geometries, where the confinement is so strong in one or two spatial directions that at low temperatures the transversal motion is "frozen" and does not contribute to the dynamics of the system. The mean-field energy, due to binary interparticle interactions, becomes smaller than the typical trapping energy in these directions. In this way, dilute repulsive BEC's have been realized in one dimension (1D) and 2D on ^{23}Na [14] and in 1D on ^{7}Li [15]. Another trend is the study of the creation of elementary excitations (vortices, solitons, and phonons) and dissipation in BEC's. The critical velocity and dissipation in these systems were studied theoretically [16,17] and experimentally first by Raman *et al.* [18] by moving a focused laser beam through a cigar-shaped repulsive BEC.

In recent experimental developments, vortices were realized in repulsive BEC's [19,20], while gray solitons have been generated in 3D repulsive BEC's by phase imprinting techniques on sodium ^{23}Na [21] and on rubidium ^{87}Rb [22]. Theoretically, gray solitons and phonons creation by a potential obstacle moving at a uniform speed in a quasi-1D infinite fluid have also been studied [23–25]. Early confining traps were well approximated by harmonic potentials [11–13], but more general ones are now in use [26]. Very recently, the dynamical evolution of a repulsive BEC confined in a quasi-1D static nonharmonic trap has been numerically studied and revealed that the reflection of a gray soliton by the

*Electronic address: azizrad@hotmail.com and radouani@lps.ens.fr

parabolic boundaries of the nonharmonic trap gives rise to the emission of phonons [27,28]. In the present work, we consider a very elongated dilute repulsive BEC confined in a static nonharmonic trap. In order to create elementary excitations of soliton and phonon types, we stir this trapped condensate by an oscillating Gaussian obstacle (an external localized repulsive potential). The speed of the obstacle through the condensate is constant but its direction reverses periodically. We numerically solve the 1D GPE that describes the dynamical evolution of this trapped condensate and investigate the superfluidity and dissipation in this quasi-1D trapped condensate at different constant obstacle velocities.

This work is organized as follows: In Sec. II, the model describing the dynamical evolution of the trapped quasi-1D BEC stirring with the oscillating obstacle in the Gaussian form and the numerical procedure are presented. Our numerical results are presented in Sec. III. They consist in the identification of elementary excitations created by the motion of the oscillating Gaussian obstacle through the quasi-1D trapped BEC and in the exploration of superfluid and dissipative behaviors of this condensate for different obstacle velocities. Section IV is devoted to a discussion of these results and to the conclusions of the present work.

II. DYNAMICAL DESCRIPTION

A. Model and oscillating obstacle

The dynamical evolution of the condensate wave function can be accurately modeled by the usual dimensionless 1D GPE:

$$i\partial_t A = -\partial_{xx}A - A + |A|^2 A + U(x,t)A, \tag{1}$$

where A is the complex field amplitude of the condensate wave function, $\rho=|A|^2$ the time-dependent density of the condensate (with $N=\int dx|A|^2$ the total number of atoms in the trapped BEC), and $U(x,t)$ the 1D static nonharmonic trap $V(x)$ superimposed upon the time-dependent oscillating Gaussian obstacle $W(x,t)$ with $U(x,t)=V(x)+W(x,t)$. We choose $V(x)$ as a flat potential with parabolic boundaries:

$$V(x)=\begin{cases}\left(\dfrac{x-x_1}{L}\right)^2 & \text{for } 0\leqslant x\leqslant x_1,\\ 0 & \text{for } x_1\leqslant x\leqslant (l-x_1),\\ \left(\dfrac{x-l+x_1}{L}\right)^2 & \text{for } (l-x_1)\leqslant x\leqslant l,\end{cases} \tag{2}$$

where l is the width of $V(x)$ (l is larger than x_1, $x_1=27$, $l=200$) and L (length, $L=6.9$) characterizes the smoothness of $V(x)$. The oscillating Gaussian obstacle $W(x,t)$, initially centered at x_0, is expressed as

$$W(x,t)=W_0\exp\left[-\left(\frac{x-x(t)-x_0}{\sigma}\right)\right], \tag{3}$$

where W_0 and σ are the obstacle depth and width, respectively. The oscillatory uniform motion of the $W(x,t)$ is obtained by taking $x(t)$ in the following triangular form as a function of the time t:

$$x(t)=\begin{cases}v\left(t-\dfrac{n}{f}\right) & \text{for } 0<\left(t-\dfrac{n}{f}\right)<\dfrac{1}{2f},\\ -v\left(t-\dfrac{n}{f}\right)+4\alpha & \text{for } \dfrac{1}{2f}<\left(t-\dfrac{n}{f}\right)<\dfrac{1}{f},\end{cases} \tag{4}$$

where n is the number of completed oscillations, α is the amplitude (half of the distance between motion extrema), and v, expressed as $v=4\alpha f$, is the constant obstacle velocity. We note that $W(x,t)$ represents the laser beam used in the experiment of Raman *et al.* [18]. For this 1D description to be valid, the healing length ξ of the condensate must larger than the mean interparticle separation $1/\rho$ along the x axis of the BEC—i.e., $\rho\xi\gg 1$—and also larger than the mean half radial width $R_\perp$ of this elongated BEC—i.e., $\xi\gg R_\perp$ [27,29].

B. Numerical procedure

We present briefly our numerical procedure. The initial condition is built from the ground state of the 1D GPE [Eq. (1)] which is the stationary solution A_0 of this equation with a stationary Gaussian obstacle $W(x,0)$ at $t=0$. It is obtained by minimizing the Gross-Pitaevskii energy functional H associated with Eq.(1):

$$H=\int dx\left[|\nabla A|^2+\frac{1}{2}(|A|^2-1)^2+U(x,0)(|A|^2-1)\right]. \tag{5}$$

The minimization of H is performed by integrating to relaxation the 1D real Ginzburg-Landau equation (RGLE) [with $U(x,0)=V(x)+W(x,0)$]

$$\partial_t R=-\partial_{xx}R-R+R^2R+U(x,0)R, \tag{6}$$

starting from an initial condition $\gamma(x)$ of the Gaussian form with

$$\gamma(x)=\gamma_0\left\{\exp\left[-\left(\frac{x-x_0}{\sigma_1}\right)^2\right]\right\},$$

with $\gamma_0=0.5$, $x_0=100$, and $\sigma_1=30$. This provides the real and stable ground-state wave function R_0, which constitutes our initial condition $A_0(A_0=R_0)$. A finite-difference Crank-Nicholson scheme is then used to evolve Eq. (1) starting from this initial condition. We checked that the total number of atoms in the trapped condensate is conserved for all our numerical results.

III. NUMERICAL RESULTS

The shape of $W(x,t)$ varies with the parameters W_0 and σ as can be seen from Eq. (3), whereas the value of its velocity v depends on amplitude α and frequency f (with $v=4\alpha f$). The 1D GPE [Eq. (1)] has been integrated at various frequencies associated with different obstacle velocities and for different obstacle parameters W_0 and σ. In Fig. 1, we first present numerical solutions of Eq. (1) (with $W_0=0.5$, $\sigma=5$, and $\alpha=5$) at four frequencies associated with different obstacle velocities, $v=0.16$, 0.625, 1.40, 3.36. As expected for obstacle velocities v below a critical value v_c (e.g., for $v=0.16$, $v_c=0.28$), the oscillatory uniform motion of $W(x,t)$

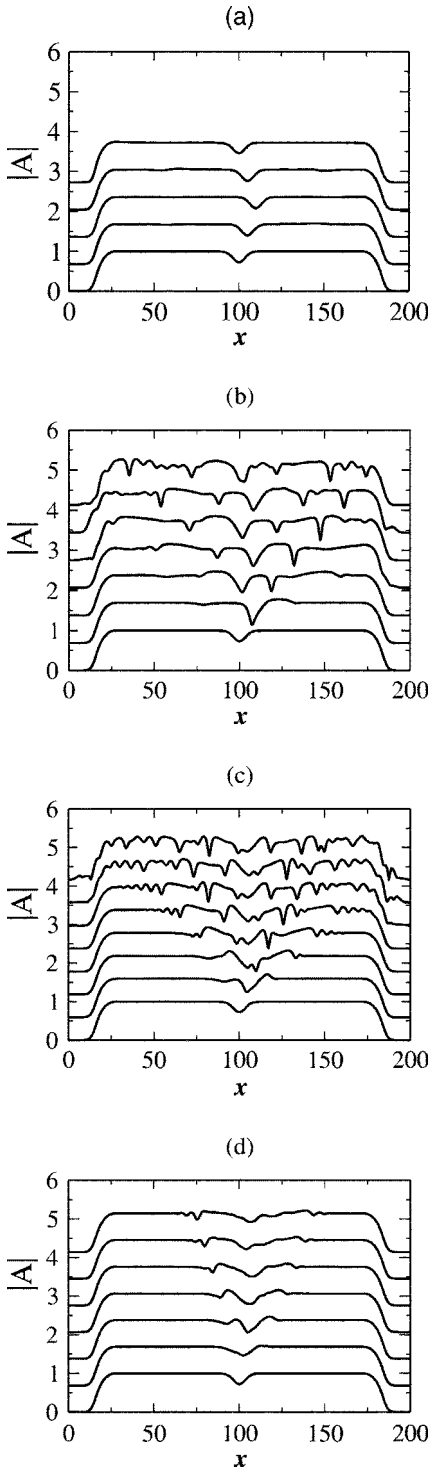

FIG. 1. Solution modulus $|A|$ of Eq. (1) (with $W_0=0.5$, $\sigma=5$, and $\alpha=5$) obtained at four frequencies $f=0.0080$, 0.03125, 0.0700, and 0.1666 which correspond to the constant obstacle velocities $v=0.16$, 0.625, 1.40, and 3.36, respectively. These four figures, in which $|A|$ is plotted as a function of position x, indicate that the oscillatory obstacle motion ($v=0.16$, $v_c=0.28$, where v_c is the critical velocity) does not create excitations for $v<v_c$ (a), but that this motion produces elementary excitations of gray soliton and phonon types for $v>v_c$: $v=0.625$ (b) and $v=1.40$ (c). We note that these excitations disappear progressively at high obstacle velocities—for example, $v=3.36$ (d).

produced almost no excitations in the condensate [Fig. 1(a)]. In contrast, when v exceeds v_c, the obstacle uniform motion produces gray solitons and phonons which are successively emitted to the right and left of the obstacle [Figs. 1(b) and 1(c)]. We note that the soliton velocities are greater than that of the obstacle [for example, in Fig. 1(b), $v=0.625$, $v_{soliton}=0.92$]. The increase of v first leads to the increase of total emission of solitons and phonons [Fig. 1(c)] as previously reported in 2D and 3D repulsive condensates. However, further increase in v reveals a different phenomenon. When v exceeds a given value ($v=1.4$ for Fig. 1), gray soliton emission reaches a maximum at $v=1.4$ [Fig. 1(c)] and then disappears progressively [Fig. 1(d)], and finally almost completely vanishes at high velocities ($v=4,5,10$). The progressive disappearance of gray solitons in the condensate depends on the obstacle velocity and is accompanied by an increase of emitted phonons. This numerical observation can be partially understood by taking into account the relation between the depth λ of a gray soliton and its velocity $c^2+\lambda^2=2$ (see Ref. [27]). This indicates that a gray soliton which is steady in the obstacle frame disappears for $\lambda=0$ and transforms into phonons, because its velocity c exceeds the speed of sound defined as $c_s=\sqrt{2}$ [Fig. 1(d)].

As for phonons, the emission first is only due to the abrupt change of the obstacle velocity at motion extrema; then, it increases with the increase of v and finally also completely disappears at high velocity.

In order to further quantify these results and investigate dissipation at different obstacle velocities and for various parameter values of W_0 and σ, we have computed both the total energy E of the condensate [Eq. (5)] and the associated mean rate of energy dissipation $\langle dE/dt\rangle$ for different obstacle velocities. This mean rate is obtained by a linear regression analysis of the energy-time data and represents the variation in time of the condensate total energy. In Fig. 2, we plotted $\langle dE/dt\rangle$ associated with different obstacle velocities (black circles) and for $W_0=0.5$, $\sigma=5$, and $\alpha=5$. This figure shows that below a critical velocity $v_c=0.28$, the total energy E remains constant in time ($\langle dE/dt\rangle\simeq 0$). But for $v>v_c$, $\langle dE/dt\rangle$ increases approximately linearly with v, attains an upper limit, and then decreases and vanishes at high obstacle velocities. The decrease of $\langle dE/dt\rangle$ is exponential for high obstacle velocities, as can be seen in the inset of Fig. 2.

In order to make contact with previous results, we first examine the dependence of $\langle dE/dt\rangle$ and the critical velocity v_c on the depth W_0 and separately on the width σ of the oscillating obstacle $W(x,t)$ (with $W_0<1$). We plot in Fig. 3 the energy increase as a function of obstacle velocity v for $W_0=0.30$, 0.50, 0.75 (with $\sigma=5$ and $\alpha=5$). The figure shows that the dissipation in the condensate increases with an increase of the obstacle depth W_0. The critical velocity value associated with every curve ($v_c=0.10,0.28,0.47$) can be evaluated by extrapolation. The critical velocity is found to depend on W_0. In the inset, W_0 is plotted as a function of v_c by using directly the preceding evaluated values of W_0 and v_c. The different values obtained are compared to a previous prediction valid for $W_0<1$ and $\sigma\gg 1$ [23]:

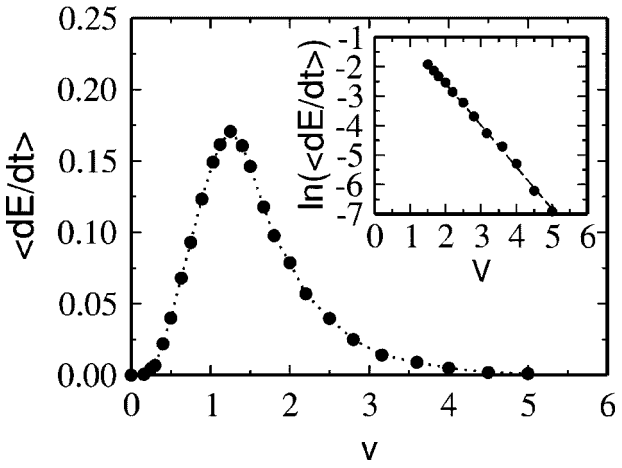

FIG. 2. The mean rate $\langle dE/dt\rangle$, which represents the increase of the condensate energy by the oscillating obstacle motion, is plotted as a function of different constant obstacle velocities (black circles), with $W_0=0.5$, $\sigma=5$, and $\alpha=5$. This figure shows that $\langle dE/dt\rangle \simeq 0$ for velocity values v below a critical velocity $v_c=0.28$. For $v>v_c$, it increases approximately linearly with the increase of v, attains its upper limit, and then decreases progressively and tends to zero at high obstacle velocities ($v>4$). The decrease of $\langle dE/dt\rangle$ with the increase of v is exponential as shown in the inset.

$$W_0 = \frac{v^2}{4} - \frac{3}{2}\left(\frac{v^2}{2}\right)^{1/3} + 1. \tag{7}$$

This inset illustrates that the numerically values obtained of W_0 and v_c are in good agreement with those theoretically predicted by Eq. (7).

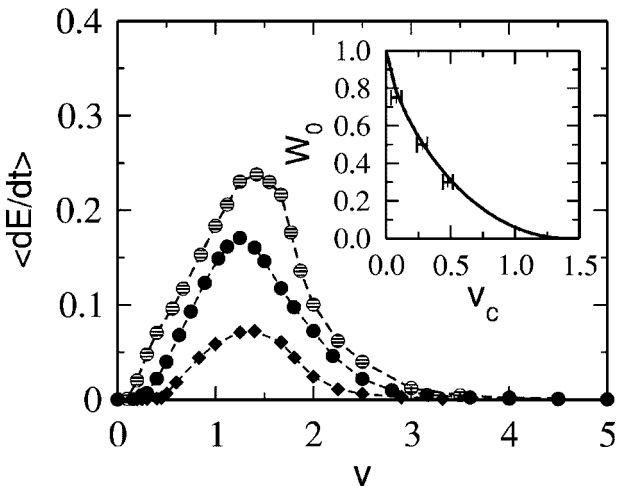

FIG. 3. Dependence of the mean rate $\langle dE/dt\rangle$ and critical velocity v_c on the depth $W_0<1$ of the oscillating obstacle $W(x,t)$ for fixed width $\sigma\gg 1$ and amplitude $\alpha>2$ (here $\sigma=5$, $\alpha=5$). We find that $v_c=0.10$ for $W_0=0.75$ (dashed circles), $v_c=0.28$ for $W_0=0.50$ (black circles), and $v_c=0.47$ for $W_0=0.30$ (black diamonds). In the inset, the preceding values (v_c with error bars) are compared to the equation $W_0=v^2/4-\frac{3}{2}(v^2/2)^{1/3}+1$. The three values of v_c directly evaluated and represented by error bars are in good agreement with those predicted theoretically (line).

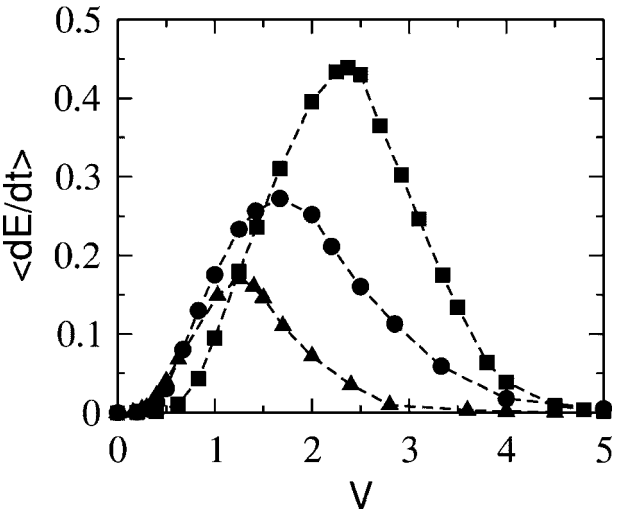

FIG. 4. Dependence of the mean rate $\langle dE/dt\rangle$ and critical velocity v_c on the width σ of the oscillating obstacle $W(x,t)$ for fixed depth $W_0<1$ and amplitude $\alpha>2$ (here $W_0=0.5$ and $\alpha=5$). The three curves correspond, respectively, to $\sigma=1$ (black squares), $\sigma=3$ (black circles), and $\sigma=5$ (black triangles). We note that the dissipation represented by $\langle dE/dt\rangle$ and the critical velocity v_c increase with the decrease of σ. The increase of σ favors the suppression of gray solitons and phonons in the condensate at high obstacle velocities.

Figure 4 represents the dependence of $\langle dE/dt\rangle$ for a fixed depth $W_0<1$ and amplitude $\alpha>2$ (here $W_0=0.5$, $\alpha=5$), on the width σ of the oscillating obstacle $W(x,t)$. In this figure, $\langle dE/dt\rangle$ is plotted as a function of the obstacle velocity v for $\sigma=1$, 3, 5. We note that as σ decreases, both the dissipation represented by $\langle dE/dt\rangle$ and the critical velocity v_c in the condensate increase. The increase of σ favors the suppression of gray solitons and phonons in the condensate at high obstacle velocities.

Analytical interpretation of emission suppression at high velocity

The exponential decrease of $\langle dE/dt\rangle$ at high obstacle velocities (see inset of Fig. 2) contrasts with previous results reported in two and three dimensions. We provide here a simple explanation of this effect modeled upon classic calculations of radiation of capillary-gravity waves by a moving obstacle [30]. An estimate of the radiation emitted by a particle is also provided in Ref. [31], but without consideration of the high-velocity behavior in 1D.

We can linearize Eq. (1) for small oscillations in the form

$$A = 1 + \eta(x,t), \tag{8}$$

where η is a small perturbation **(**$\eta \ll 1$, and $\eta(x,t) = \eta_0 \exp[i(kx-\omega t)]$**)**. This leads to the well-known dispersion relation

$$\omega = k\sqrt{k^2+2} \tag{9}$$

and provides the wave phase velocity $c(k)=\omega/k=\sqrt{k^2+2}$. Dissipation is dominated by waves that appear steady in the

obstacle frame and satisfy $c(k)=v$. This determines the wave number of the emitted phonons as

$$k=\sqrt{v^2-2}. \tag{10}$$

Now, the emission rate of phonons of wavelength k is proportional to the Fourier transform $\tilde{P}(\sigma,k)$ of the modulus of the superfluid wave function modulation $P(x/\sigma)$ due to the moving obstacle. Considering an obstacle moving at stationary speed v [23], $P(x/\sigma)$ is approximately obtained as

$$P\left(\frac{x}{\sigma}\right)\simeq\left[1-4\frac{W(x,0)}{v^2}\right]^{-1/4}. \tag{11}$$

For $v\gg\sqrt{2}$, Eq. (10) can be approximately written as $k\simeq v$, and the wavelength of the emitted phonons becomes much shorter than the length scale of the potential. So

$$\tilde{P}(\sigma,k)=\int \exp(ikx)P\left(\frac{x}{\sigma}\right)dx\propto \exp(-\beta\sigma k) \quad \text{for } k\gg 1 \tag{12}$$

or

$$\tilde{P}(\sigma,k)\propto \exp(-\beta\sigma v), \tag{13}$$

where $\beta=\sqrt{\ln(v^2/4W_0)}$ and W_0 is the prefactor of the exponential in Eq. (3). Here β depends on the shape of P and comes from the complex singularity of Eq. (11) closed to the real axis. In the range of velocities considered, β depends very weakly on v and Eq. (12) explains the exponential suppression of emission at high velocities observed in Fig. 2. It also explains why an increase in σ favors this suppression as seen in Fig. 3 since this further increases the moving potential length scale as compared to the wavelength of the emitted phonons. The estimate given by Eq. (13) is of course only valid for a smooth potential. Dissipation suppression at high velocity is much less prononced for nonsmooth potentials like those considered in Ref. [25], since their singularities lie on the real x axis.

IV. DISCUSSION AND CONCLUSION.

In this paper, we have analyzed the creation of elementary excitations produced by an oscillating obstacle through a quasi-1D trapped repulsive Bose condensate. We have shown that the creation of excitations, gray solitons, and phonons depends on the obstacle velocity and on the obstacle shape. We have confirmed previous calculations of critical velocities in 1D [23]. We have found that the dissipation increases with the increase of the obstacle velocity value, like in the case of the formation of vortices previously studied [17,18], but contrarily to the case of vortices, we have found that it attains an upper limit and then decreases exponentially with the obstacle velocity increase. At high obstacle velocity, the dissipation vanishes and the repulsive condensate behaves as a quasisuperfluid. This absence of dissipation already noted in Ref. [25] is reminiscent of that previously described for the motion of a smooth potential with $\sigma\gg 1$ [32] at fixed velocity as interpreted in Ref. [33]. In both cases, dissipation suppression comes because the wavelength of the emitted phonons is short compared to that of the stirring potential.

ACKNOWLEDGMENTS

This work was performed in the Laboratoire de Physique Statistique de l'Ecole Normale Supérieure, Paris, France. With great and special pleasure, we thank V. Hakim for instructive and valuable scientific discussions. We also wish to thank A. Boudaoud and B. Echebarria for scientific discussions and V. Bretin and D. Guéry-Odelin for informing us on their ongoing experiments. We acknowledge the hospitality of LPS and of its director J. Meunier.

[1] J. F. Allen and A. D. Misen, Nature (London) **141**, 75 (1938); P. L. Kapitza, *ibid.* **141**, 74 (1938).
[2] L. D. Landau, J. Phys. (Moscow) **5**, 71 (1941); I. M. Khalatnikov, *Introduction To the Theory of Superfluidity* (Addison-Wesley, Redwood City, CA, 1989).
[3] N. N. Bogoliubov, J. Phys. (Moscow) **11**, 23 (1947).
[4] R. P. Feynman, Prog. Low Temp. Phys. **1**, 17 (1955).
[5] M. H. Anderson, J. R. Ensher, M. R. Matthews, C. E. Wieman, and E. A. Cornell, Science **269**, 198 (1995).
[6] K. B. Davis, M. O. Mewess, M. R. Andrews, N. J. Van Druten, D. S. Durfee, D. M. Kurn, and W. Ketterle, Phys. Rev. Lett. **75**, 3969 (1995).
[7] C. C. Bradley, C. A. Sakett, J. J. Tolett, and R. G. Hulet, Phys. Rev. Lett. **75**, 1687 (1995); C. C. Bradley, C. A. Sakett, and R. G. Hulet, *ibid.* **78**, 985 (1997).
[8] M. R. Andrews, C. G. Townsend, H. J. Miesner, D. S. Durfee, D. M. Kurn, and W. Ketterle, Science **275**, 637 (1997).
[9] E. A. Burt, R. W. Ghrist, C. J. Myatt, M. J. Holland, E. A. Cornell, and C. E. Wiemen, Phys. Rev. Lett. **79**, 337 (1997).
[10] E. P. Gross, Nuovo Cimento **20**, 454 (1961); L. P. Pitaevskii, Zh. Eksp. Teor. Fiz. **40**, 646 (1961) [Sov. Phys. JETP **13**, 451 (1961).
[11] W. P. Reinhardt and C. W. Clark, J. Phys. B **30**, L785 (1997).
[12] F. Dalfovo, S. Giorgini, L. P. Pitaevskii, and S. Stringari, Rev. Mod. Phys. **71**, 463 (1999).
[13] Th. Busch and J. R. Anglin, Phys. Rev. Lett. **11**, 2298 (2000).
[14] A. Gorlitz, J. M. Vogels, A. E. Lenhardt, C. Raman, T. L. Gustavson, J. R. Abo-Shaeer, A. P. Chikkatur, S. Gupta, S. Ionouye, T. Rosenband, and W. Ketterle, Phys. Rev. Lett. **87**, 130402 (2001).
[15] F. Schreck *et al.*, Phys. Rev. Lett. **87**, 080403 (2001).
[16] T. Frisch, Y. Pomeau, and S. Rica, Phys. Rev. Lett. **69**, 1644 (1992).
[17] J. B. Jackson, J. F. McCann, and C. S. Adams, Phys. Rev. A **61**, 051603 (2000).
[18] C. Raman, M. Kohl, R. Onofrio, D. S. Durfee, C. E. Kuklewicz, Z. Hadzibabic, and W. Ketterle, Phys. Rev. Lett. **83**, 2502 (1999).

[19] M. R. Matthews *et al.*, Phys. Rev. Lett. **83**, 2498 (1999).
[20] K. W. Madison *et al.*, Phys. Rev. Lett. **84**, 806 (2000).
[21] J. Denschlag *et al.*, Science **287**, 97 (2000).
[22] S. Burger *et al.*, Phys. Rev. Lett. **83**, 5198 (1999).
[23] V. Hakim, Phys. Rev. E **55**, 2835 (1997).
[24] P. Leboeuf and N. Pavloff, Phys. Rev. A **64**, 033602 (2001).
[25] N. Pavloff, Phys. Rev. A **66**, 013610 (2002).
[26] V. Bretin, J. Dalibard, and S. Stock (private communication).
[27] A. Radouani, Phys. Rev. A **68**, 043620 (2003).
[28] N. G. Parker, N. P. Proukakis, M. Leadbeater, and C. S. Adams, Phys. Rev. Lett. **90**, 220401 (2003).
[29] D. S. Petrov, G. V. Shlyapnikov, and J. T. M. Walraven, Phys. Rev. Lett. **85**, 3745 (2000).
[30] G. B. Whitham, *Linear and Nonlinear Waves* (Wiley-Interscience, New York, 1974).
[31] D. L. Kovrizhin and L. A. Maksimov, Phys. Lett. A **282**, 421 (2001).
[32] C. K. Law, C. M. Chan, P. T. Leung, and M.-C. Chu, Phys. Rev. Lett. **85**, 1598 (2000).
[33] M. Haddad and V. Hakim, Phys. Rev. Lett. **87**, 218901 (2000).